Space: Science & Technology
A SCIENCE PARTNER JOURNAL

REVIEW ARTICLE

Volcanism and Deep Structures of the Moon

Jiannan Zhao[1,2], Le Qiao[3], Feng Zhang[4], Yuefeng Yuan[5], Qian Huang[5], Jianguo Yan[6], Yuqi Qian[1], Yongliao Zou[4], and Long Xiao[1*]

[1]State Key Laboratory of Geological Process and Mineral Resources, Planetary Science Institute, School of Earth Sciences, China University of Geosciences, Wuhan 430074, China. [2]Key Laboratory of Geological Survey and Evaluation of Ministry of Education, China University of Geosciences, Wuhan 430074, China. [3]Shandong Key Laboratory of Optical Astronomy and Solar-Terrestrial Environment, School of Space Science and Physics, Institute of Space Sciences, Shandong University, Weihai, Shandong 264209, China. [4]State Key Laboratory of Space Weather, National Space Science Center, Chinese Academy of Sciences, Beijing 100190, China. [5]Hubei Subsurface Multi-scale Imaging Key Laboratory, Institute of Geophysics and Geomatics, China University of Geosciences, Wuhan 430074, China. [6]State Key Laboratory of Information Engineering in Surveying, Mapping and Remote Sensing, Wuhan University, 129 Luoyu Road, Wuhan 430070, China.

*Address correspondence to: longxiao@cug.edu.cn

Citation: Zhao J, Qiao L, Zhang F, Yuan Y, Huang Q, Yan J, Qian Y, Zou Y, Xiao L. Volcanism and Deep Structures of the Moon. *Space Sci. Technol.* 2023;3:Article 0076. https://doi.org/10.34133/space.0076

Submitted 18 April 2023
Accepted 5 September 2023
Published 11 October 2023

Copyright © 2023 Jiannan Zhao et al. Exclusive licensee Beijing Institute of Technology Press. No claim to original U.S. Government Works. Distributed under a Creative Commons Attribution License 4.0 (CC BY 4.0).

Volcanism is the most important endogenic geological process of the Moon, which is closely related to its internal structure and thermal history. Lunar volcanism is one of the most important topics for lunar science and explorations. Recent lunar orbital observations, in situ explorations, and sample return missions have returned a new generation of high-resolution datasets, which greatly enriched our knowledge of lunar volcanism. Here, we summarize recent advances in the duration and spatial distribution of lunar mare volcanism, as well as origin of volcanic landforms such as lava flows, sinuous rilles, lava tubes, domes, and cones. We proposed several outstanding problems in the study of temporal and spatial span of lunar volcanism, the formation mechanism of the varied volcanic landforms, and their relation with deep structures. To solve these problems, more in situ explorations and sample return missions from various volcanic units are needed.

Downloaded from https://spj.science.org on October 31, 2023

Introduction

As a fundamental geological process of the Moon, volcanism has played an important role in shaping the lunar surface, leading to the formation of a variety of volcanic landforms such as lunar maria, lava flows, sinuous rilles, domes, cones, etc. [1]. Moreover, volcanism is closely related to its deep structures, and geological and thermal history, and therefore has always been the focus of lunar science and explorations.

The study of lunar volcanism begins before the space age. At the time, humans could only observe the nearside of the Moon through eyes or ground-based telescopes, and found that many impact basins on the lunar nearside were filled with massive dark deposits now known as mare basalts [2]. Volcanism on the lunar farside was unknown until orbital data were obtained. In 1959, the Soviet Luna 3 probe photographed the lunar farside for the first time, and revealed that very few mare basalts occur in large impact basins there [3], a distribution pattern very different from the lunar nearside. Then, the implementation of Apollo and Luna sample return missions provided us opportunities to study the property of lunar volcanism through direct analyses of lunar samples [4–6]. In the last 3 decades, a series of lunar exploration missions such as Clementine [7], Lunar Prospector [8], SELENE [9], Lunar Reconnaissance Orbiter [10,11], Gravity Recovery and Interior Laboratory (GRAIL) [12], Chandrayaan missions [13,14], and Chang'e missions [15–21] have acquired masses of lunar remote sensing and in situ data as well as returned samples, which have greatly improved our understanding of lunar volcanism [22,23].

Fundamental questions about relationships between the surface manifestations and deep structures of lunar volcanism still exist [24,25]. Detailed investigations on the volcanic landforms and subsurface volcanic structures will help clarify their relationship and better understand the origin and evolution of lunar volcanism as well as the Moon. Meanwhile, as the fourth stage of China's lunar exploration mission has been engaged [26], it is necessary to summarize the current research status of lunar volcanism to better prepare for future lunar missions. Therefore, in this paper, we summarized recent advances in the study of lunar volcanism, volcanic landforms, and related deep structures, and proposed several outstanding questions on this topic, hoping that they could be answered by future lunar explorations.

Distribution and Duration of Lunar Mare Volcanism

Based on the latest mapping of lunar mare deposits (Fig. 1) [27], we determined the surface area of all exposed lunar maria

as about 6.15×10^6 km^2, which accounts for ~16% of the surface area of the entire Moon. Among them, 92.9% or 5.71×10^6 km^2 of mare deposits occur in the lunar nearside, while the lunar farside maria only accounts for 7.1% of the whole mare surface area. The apparent dichotomy in the distribution of basalts on the lunar nearside and farside is mainly attributed to the relatively thicker lunar farside crust [28], which prohibited the ascent and eruption of magma [25]. The South Pole–Aitken (SPA) basin, one of the major terranes of the lunar farside, is characterized by a thin crust and thus becomes the major site of volcanism on the lunar farside. Mare basalts exposed in the SPA basin have a total surface extent of 1.66×10^5 km^2, accounting for 37.9% of the basalts of the lunar farside (Fig. 1). The SPA basin also hosts most of the regionally extensive mare deposits on the lunar farside, such as those emplaced on the floor of the Von Kármán crater where China's Chang'e-4 (CE4) mission landed [29].

Analyses of the high-resolution imaging data of the lunar surface using the crater size-frequency distribution method [30] have revealed abundant information concerning the chronology of lunar mare volcanism. We compile the crater counting results for the global distribution of nearly 500 mare basalt units on the Moon (Fig. 2), and find that the oldest exposed basalts on the lunar surface were emplaced about 4 billion years (Ga) ago, corresponding to the terminal stage of large basin-formation period in lunar history. The evidence for the oldest mare basalt clasts is revealed by the analysis of the meteorite with an age of ~4.35 Ga [31]. There are also many old mare deposits (named cryptomaria; [32] and references therein) buried by large impact basin ejectas, and hence multiple lines of evidence support that the basaltic volcanism should have started soon after the late stage of the lunar magma ocean solidification [5].

The most active period of lunar volcanism was about 3.3 to 3.8 Ga ago. During this relatively short period of about 500 million years, ~70% of the total lunar basalt unit populations were emplaced, coinciding with isotope dating results of the basaltic samples returned by Apollo and Luna missions [33]. After that, volcanic eruptions on the Moon waned sharply in middle lunar history and ceased sometime in the last ~1 Ga (Fig. 2) [34–36]. Although the spatial extent of volcanism on the lunar farside accounts for less than one-tenth of the global lunar volcanism, the general temporal extent and evolution history of farside volcanism are comparable with that of the nearside volcanism: climax at 3.3 to 3.8 Ga ago and cessation at about 1.5 Ga ago, indicating that the nearside and farside lunar volcanism are both affected by the continued cooling and contraction of the entire Moon. In addition, many young mare deposits were emplaced in the SPA basin, such as those within the Apollo basin, which have been dated as about 2.5 Ga, much younger than the basalts returned by Apollo and Luna missions.

Styles of Lunar Volcanism and Related Volcanic Landforms

Intrusive magmatism

Intrusive magmatism happens when dikes with medium overpressurization values propagate to the vicinity of lunar surface and form intrusions without erupting to the surface [25,37]. These subsurface intrusion structures may lead to the bending and fracturing of lunar surface, forming intrusive volcanic constructs such as floor-fractured craters and intrusive domes.

Floor-fractured craters

The floor-fractured crater (FFC) is a special type of impact craters on the Moon with wide-distributed fracture systems on its floor (Fig. 3A). The fractures could be radial, concentric, or polygonal in their patterns, and some related landforms such as moats, ridges, and irregular mare patches can

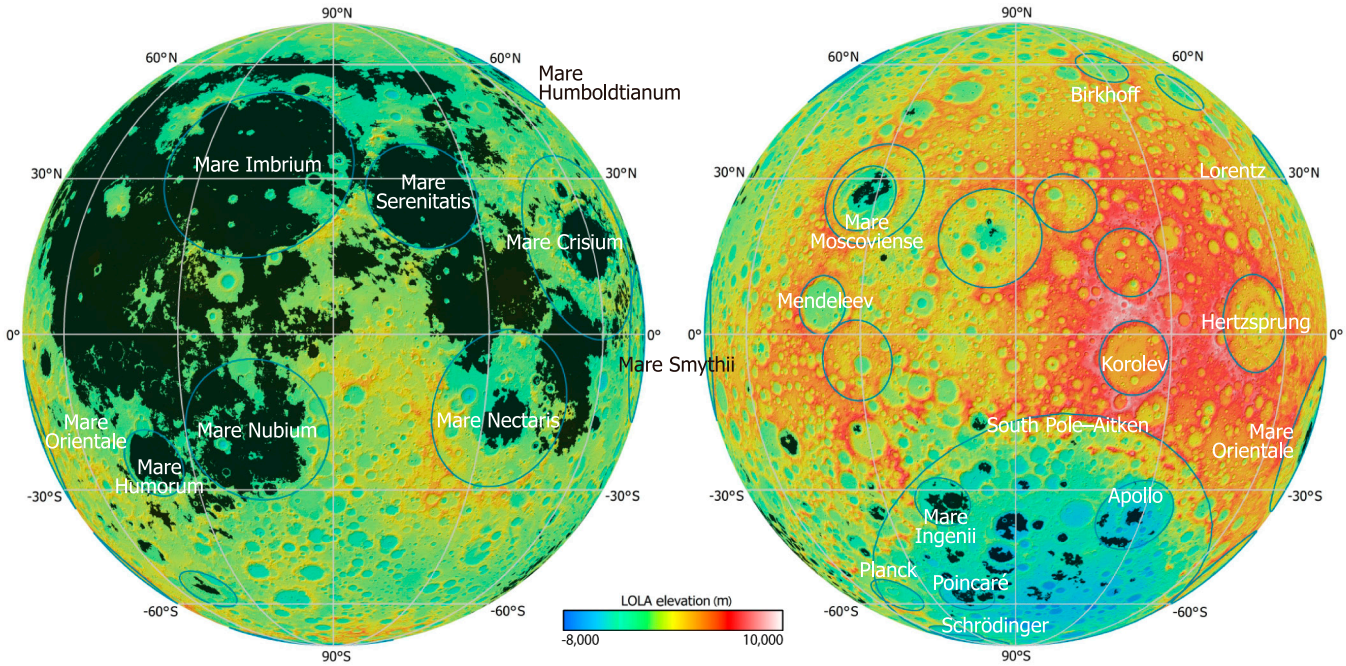

Fig. 1. Maps of the lunar nearside (left) and farside (right) showing the spatial distribution of mare basalts (dark gray areas, based on Nelson et al. [27]). Basemap is a colorized Lunar Orbiter Laser Altimeter (LOLA) topography overlain on LOLA hillshade, and the blue circles indicate impact basins >300 km in diameter (based on Head et al. [150]).

Downloaded from https://spj.science.org on October 31, 2023

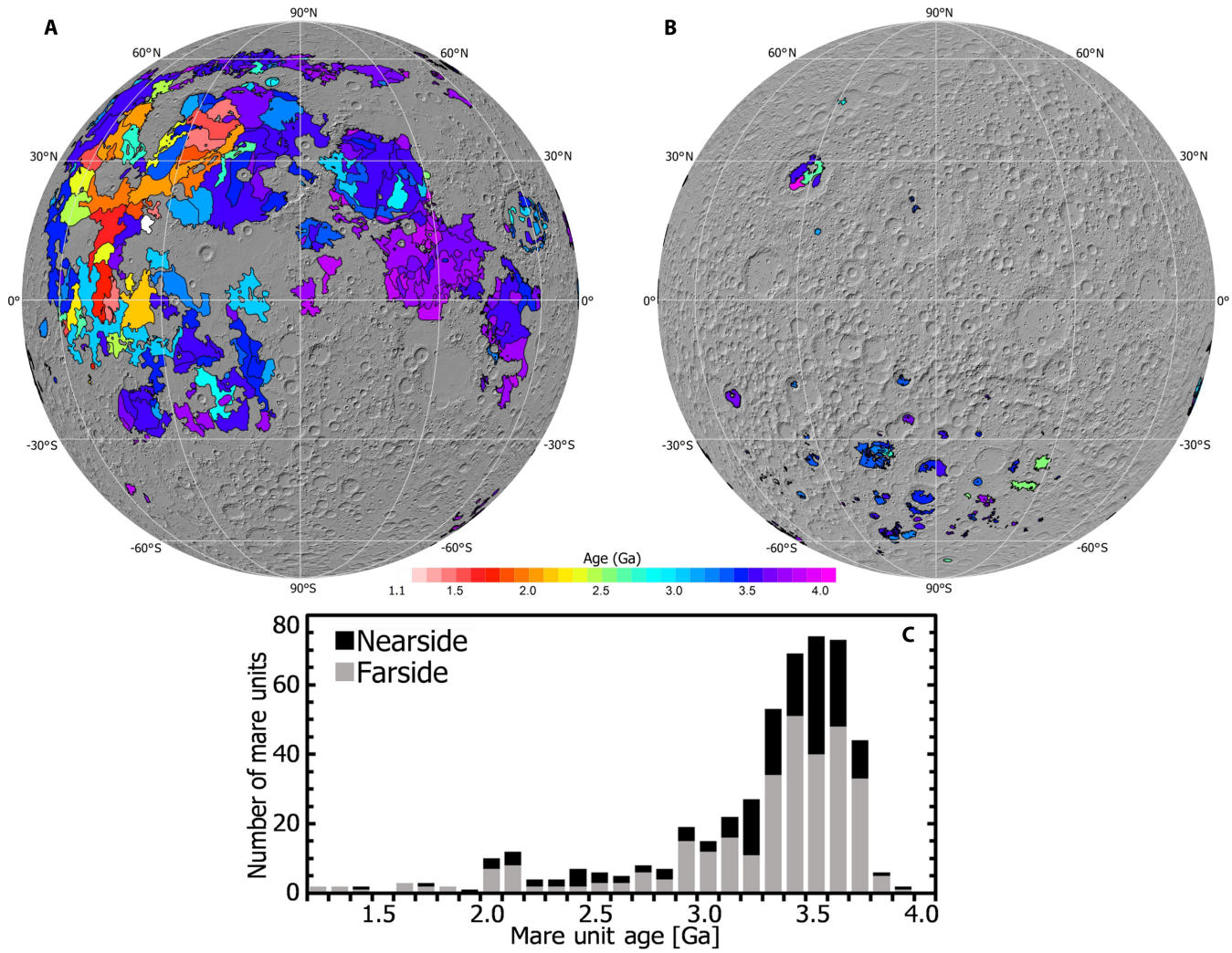

Fig. 2. Maps of the model ages of lunar nearside (A) and farside (B) mare basalt units derived from crater population measurements and the histogram (C). The mare age data are from Qiao et al. [59] and Qian et al. [34], and references therein.

develop on the floor of FFCs [38]. Based on these morphological features, Jozwiak et al. [38] divided FFCs into 6 classes. They have also studied the global distribution of FFCs, and found that most FFCs are located near lunar maria or mare-filled impact basins, although large numbers of them have also been identified in the SPA basin and lunar highlands [38]. Currently, research on FFCs is focused on their formation mechanisms and 2 main hypotheses have been proposed [37,39]. The first one is the viscous relaxation model, which suggests that the fractures form due to upward flexure of the bottom of the crater floor when high thermal gradients exist below the crater and lead to the relaxation in the regional topography [39,40]. The other one is the magmatic intrusion hypothesis, in which fractures form when magma intrudes upwards, forms a sill beneath the crater, and lifts the bottom of the overlying crater [37,41,42]. However, evidence supporting the viscous relaxation hypothesis is marginal, while the magma intrusion hypothesis has been supported by geomorphological [43], gravitational [44,45], and mineralogical [46] studies.

Intrusive domes

Lunar domes are convex-up shaped with circular or irregular outlines, and are widely distributed in lunar maria, volcanic complexes, or near the mare-highland boundary (Fig. 3D) [47]. They can be classified into effusive domes and intrusive domes based on their origins, and the latter is related to the vertical uplift of the lunar crust induced by laccolithic intrusions [48]. Intrusive domes usually have low slopes of less than 1° and can be more than 30 km in diameter according to the investigations of 10 candidate intrusive domes by Wöhler and Lena [48]. These domes are mainly located near the border of mare regions. Besides, intrusive domes may also exist in some volcanic complexes such as the Mons Rümker region based on the identification of some shallow domes [49]. However, shallow domes could also be formed by effusive eruption of low-viscosity lava, and more evidence is still needed to confirm the intrusive origin of these domes.

Effusive volcanism

The samples collected by Apollo missions confirmed the basaltic and ancient nature of the lunar maria [5], which are large basaltic plains mainly formed in volcanic effusive episodes. Mare volcanism is fed by buoyant dikes propagating upward from deep mantle partial melt sources. The geophysical models predict that when eruptions can occur, the typical magma rise

Downloaded from https://spj.science.org on October 31, 2023

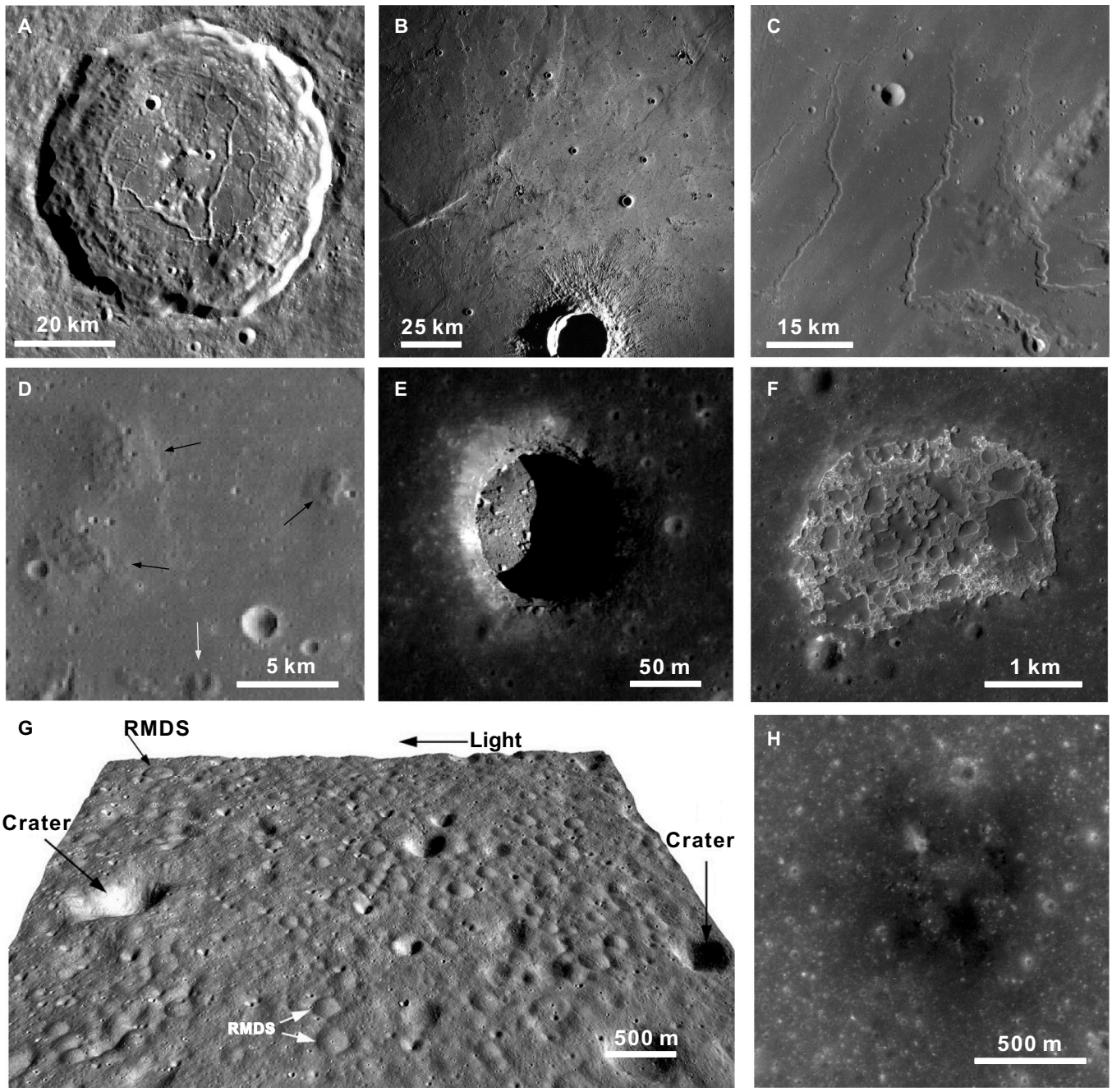

Fig. 3. Lunar volcanic landforms. (A) Floor-fractured crater (44.3°E, 46.5°N), LRO WAC mosaic. (B) Lava flows in the southwestern Imbrium (330.4°E, 25.5°N), Apollo photograph AS15-M-1701. (C) Sinuous rille (315.7°E, 27.3°N), LRO WAC mosaic. (D) Lunar dome (black arrows) and cone (white arrow) (303.6°E, 12.5°N), LRO WAC mosaic. (E) Lunar skylight (33.2°E, 8.3°N), LRO NAC image M126710873RC. (F) Irregular mare patch (IMP; 5.3°E, 18.7°N), LRO NAC image M190566313LC. (G) 3D view of ring moat dome structures (RMDSs; 30.8°E, 10.4°N), LRO NAC images M1096293859RC and M1096293859LC. (H) Pyroclastic deposits (352.2°E, 6.2°N), LRO NAC image M1103616897RC.

speeds are ~10 to tens of m s^{-1}, dike widths are of order 100 m, and eruption rates from 1- to 10-km-long fissure vents are of order 10^4 to 10^6 m^3 s^{-1} [37]. These values are huge compared to typical terrestrial eruptions and help to explain many unusual characteristics of lunar basaltic eruptions.

On the Moon, a volcanic event often includes a sequence of eruptive processes but always with overpressured volatile-rich explosive-style eruptions at the beginning due to low gravity and negligible atmospheric pressure [50]. With decreasing pressure and release of volatiles, the explosive–effusive transition always occurs. The emplacement of basaltic magmas with low viscosity is fed by dike-feeding conduits and results in the formation of various volcanic features on the lunar surface, including lava flows, lava channels, pit craters, cones, domes, etc. that are commonly seen on Earth [25].

Lava flows

The large impact basins on the Moon are flooded by voluminous basaltic lava flows with some characterized by clear flow margins that are traceable for hundreds of kilometers [51–53].

Downloaded from https://spj.science.org on October 31, 2023

For example, the Apollo photo of the surface in southwestern Imbrium shows 3 phases of young, fairly pristine mare lava flows (Fig. 3B). The 3 eruptive episodes produced flows that respectively traveled 400, 800, and 1,200 km from the vent [51]. Using crater counting methods, they were estimated to have formed ~2.0 to 3.0 Ga ago [54,55], with thicknesses varying from ~10 to 40 m [56]. Typical eruption rates are predicted to lie in the range from 10^4 to 10^6 m^3 s^{-1} with the resulting flows commonly 10 to 20 km wide, >10 m thick, and hundreds of kilometers in length [37]. As the flows advance on the lunar surface, the cooling mechanism includes radiation of the flow top and the underlying conduction between the flow bottom and the substrate. Thus, the thickness of the flows' outermost shell, i.e., the thermal boundary layer, will increase with time. The very low viscosity and highly fluid properties of lunar basaltic lava favor initial emplacement as thin, rather than thick sheets of lava. In addition to the styles and rates of eruptions that fundamentally control lava flow morphology [43], the thickness and behavior of the solidifying crust (bending, disrupting, or cracking) exert important control over the final flow appearance [25,57].

Sinuous rilles

When the magma effusion flux is very high (10^4 to 10^5 m^3 s^{-1}), long-duration (~100 to 300 days) effusive eruptions would lead to significant substrate thermal erosion and result in the formation of lunar sinuous rilles (Fig. 3C). Hurwitz et al. [58] conducted a global search of lunar sinuous rilles using high-resolution imaging and topographic data obtained by the Kaguya and LRO spacecraft, and identify more than 200 lunar sinuous rilles. These rilles vary in length from 2 km to 566 km, in width from 160 m to 4.3 km, in depth from 4.8 m to 534 m, and in sinuosity index from 1.02 to 2.1. Oceanus Procellarum contains nearly half (48%) of the catalogued sinuous rilles. Hurwitz et al. [58] also constrained the timing of the formation of lunar sinuous rilles and found that most of them were formed between 3.0 and 3.8 Ga ago, coinciding with the climax of global volcanism. The youngest sinuous rilles occur in the Aristarchus Plateau area, which may have formed 1.0 to 1.5 Ga ago.

Volcanic cones and effusive domes

Effusive domes and cones (Fig. 3D) are small volcanic edifices that are usually concentrated in volcanic complexes such as Marius Hills, Aristarchus, Mons Rümker, Gardner, etc., although they have also been identified in lunar mare surface or on the highlands [47,49,59–61]. In contrast to the aforementioned intrusive domes, effusive domes are usually formed when magma with high viscosity and/or low effusion rate erupts and accumulates around the effusive vent [48,49]. Compared with domes, volcanic cones usually have more steep flanks and obvious central vents. They form in strombolian-style eruptions when magma has a higher volatile content [25]. Marius Hills plateau has the highest concentration of cones on the Moon, and Wan et al. [62] identified 360 known and suspected volcanic cones in this region and classified them into 5 morphological types. Although a lot of work has been done concerning the identification, morphology, composition, and rheology of lunar domes and cones, there are still some problems that need to be solved: (a) Age determination of the domes and cones needs to be improved as they have a relatively small surface area, leading to large dating uncertainty. (b) Sample returning missions are required to clarify the formation mechanism of silicic lava dome that is a special type of lunar effusive dome with silica-rich composition that may have important implications for the lunar magma evolution [63,64]. (c) The identification and classification of lunar domes and cones should be improved based on newly acquired high-resolution morphological and topographical data [62] as well as new techniques such as machine learning [65].

Lava tubes and skylights

Lava tubes are typical volcanic features on planetary surfaces [66–68]. They were evidenced on the Moon by discontinuous pit chains [69] and vertical holes that are called "skylights" (Fig. 3E) [70,71]. Early studies proposed that sinuous rilles may have evolved into lava tubes when segments of the channels were roofed over [69]. Lunar lava tubes have been paid high attention as they are ideal sites for the construction of lunar bases because they (a) provide immense underground space for construction, which does not need to build or burrow on a large scale; (b) provide an environment that has relatively constant temperature and weak cosmic radiation, and is barely influenced by lunar dust and micrometeorite impacts; and (c) may provide necessary resources for human daily life such as water ice or other volatiles [69,72].

Irregular mare patches

Lunar Irregular Mare Patches (Fig. 3F; IMPs) [73] are a type of mare features on lunar surface with special "blistered" appearance (meniscus-like bulbous shaped mounds surrounded by rough and optically immature materials). They have aroused interest of researchers since the discovery of Ina, the most remarkable endogenic IMP feature located in Lacus Felicitatis (18.65°N, 5.30°E), by the Apollo 15 mission [74]. We compiled all previous lunar IMP identifications since the Apollo era and present an updated, comprehensive inventory of 91 lunar IMPs [59].

Although Ina could be formed in relatively recent geological time due to its crisp appearance, optical immaturity, and low number of superposed impact craters, the specific formation mechanism is still under debate. Various theories have been proposed to explain the nature and origin of lunar IMPs, including sublimation-induced high reflectance of the floor terrains [74], small lava intrusions within a collapse caldera atop an extrusive volcanic dome [75], removal of surface regolith by episodic out-gassing within the past 10 Ma [76], lava flow inflation (mounds) and subsequent lava breakout (floor hummocky terrains) [77], explosive volcanic eruptions and the resultant deposition of fine-grained, block-free pyroclastics [78], geologically very recent volcanic eruption model [73], and lava lake processes and magmatic foam extrusion [79,80]. In summary, a series of questions concerning the spatial distribution, geological context information, formation age and physical properties of lunar IMPs need to be explored by future missions and studies.

Ring moat dome structures

An enigmatic feature, named Ring Moat Dome Structure (RMDS; Fig. 3G) in the lunar maria has been noticed in the Apollo era and extensively investigated recently [57,81–83]. They often display topographic characteristics with low domical mounds surrounded by ring depressions (or moats). On

Downloaded from https://spj.science.org on October 31, 2023

average, these mounds are commonly ~200 m in diameter with a mean height of ~3 to 4 m [57]. Both isolated and clustered patterns are seen for their distribution (Fig. 3G), and at the same time, RMDSs are found to locate in various mare settings and show no distinct composition from the surrounding maria that they are located in [81]. Based on a series of observable results, in particular their spatial relationship with many volcanic features, a volcanic hypothesis has been proposed for their formation [81,83]. They are interpreted as extrusions of volatile-rich, overpressured melt in the interior of flowing lava [81,83]. Crater count dating results [81] and small crater–RMDS overlap relationship suggest that RMDS-formation-related mare volcanism might have occurred in very recent epochs of less than 1.0 Ga in the Copernican era [82]. Otherwise, RMDSs would have been erased by lunar regolith formation processes due to the impact gardening effect. However, there are no geophysical models and eruption mechanisms that can account for the very young small-scale mare volcanism to form RMDSs because, at the time, magma source regions should have moved into the deep lunar interior, and hence, it would have been very difficult for magma to reach the surface [25,57,82]. Therefore, and with more confidence, RMDSs are interpreted as an unusual manifestation of the emplacement of lavas between 3 and 4 Ga ago, during the era of mare basalts emplacement [83]. In addition, a shallow laccolith intrusion model [84] is proposed to explain their formation. However, this model also relies on volcanic activity and it is not easily consistent with the current knowledge of the thermal evolution history of the Moon [85].

Explosive volcanism

In the course of the dike propagation to the surface, volatile phases within the magma would continuously exsolve due to pressure release, generating abundant gas bubbles at the dike tip. Expansion of the bubble-rich magma into the lunar vacuum would lead to explosive eruptions and the deposition of pyroclastic materials surrounding the volcanic vent. Explosive eruptions are relatively common on the Moon, and hundreds of pyroclastic deposits have been identified on the lunar surface [86]. Similar to volcanic eruptions on Earth, lunar explosive volcanic eruptions are also modulated by magma effusion rate, physical property, and the volatile content of the magma, thus generating various kinds of eruption styles and deposition. However, due to the unique environment of the lunar surface, including the low lunar gravity and lack of an atmosphere, typical volcanic eruption styles on Earth would result in different explosive eruption types and the resultant deposits on the Moon [25].

Terrestrial Hawaiian-style eruptions occurring in the lunar environmental conditions would produce regional and localized pyroclastic deposits (Fig. 3H) [87]. Over 100 pyroclastic deposits have been identified on the lunar surface, with surface extent of up to 50,000 km^2 [86,88]. Analyses of orbital spectroscopic data can be used to constrain the crystallization and cooling rate of pyroclastic beads in these deposits [89]. For instance, pyroclastic deposits at the Aristarchus Plateau were characterized by apparent absorption features of glassy materials, indicating relatively low degree of crystallinity, while the deposits at Sinus Aestuum have the weakest glass absorption bands, consistent with a higher degree of crystallinity.

Crustal and Mantle Structures beneath Lunar Volcanic Landforms

Layered subsurface structures of mare basalts

The stacking of mare basalts develops through lunar history with younger flows overlaying on the older flows. Therefore, detecting the subsurface conditions of lunar mare basalts will help constrain the emplacement characteristics of lunar basalts as well as the evolutionary history of lunar maria.

During the Apollo missions, active source moonquake experiments were carried out at the Apollo 14, 16, and 17 landing sites to study the lunar subsurface layered structures. At the Apollo 14 landing site, the regolith is about 8.5 m thick and the underlying layer is 19 to 76 m thick [90,91]. The regolith thickness of the Apollo 16 landing site is 7 to 22 m, and the underlying strata (Cayley Formation) is 70 to 220 m thick [92]. Apollo 17, which landed in the Taurus-Littrow Valley, observed 5 different P-wave velocity interfaces at depths of 4 m, 32 m, 390 m, and 1,385 m [93]. These layered structures may represent lava flow deposits that formed during multiple episodes of volcanic activity.

Japan's Kaguya spacecraft carries a Lunar Radar Sounder that can probe to depths of up to several kilometers. It identified subsurface layers several hundred meters deep in the lunar nearside maria, indicating that basalts are up to hundreds of meters thick [94–96]. However, the vertical resolution of orbital radar is low, and more refined mare subsurface structures have been obtained by lunar penetrating radar (LPR) aboard in situ exploration rovers.

Chang'e-3 (CE3) and CE4 spacecraft respectively landed on the mare surfaces within the Imbrium basin on the lunar nearside and the Von Kármán crater on the lunar farside [97,98]. They used LPR to probe the subsurface structures deep to hundreds of meters, revealing the emplacement history of lava flows on the nearside and the farside of the Moon. In addition, the LPR profiles show deep lava flows ranging in thickness from several meters to tens of meters, even up to hundreds of meters.

In the CE3 landing area, the low-frequency LPR detected the subsurface structure of more than 300 m deep, and thus could identify buried geological units. Therefore, it is speculated that there were multiple periods of volcanic eruptions in the landing area [53,99]. The deep radar reflection resembles that of the shallow Eratosthenian basalts, possibly suggesting the youngest Imbrium basalts filling the Imbrium basin at around 3.3 Ga [99,100]. In addition, the high-frequency LPR reveals that the overall thickness of the Eratosthenian basalts is more than 30 m starting at the depths of ~10 m, which can be further divided into 3 sub-stages [101]. The overall thickness and depth ranges of the Eratosthenian mare unit in the CE3 landing region are in good agreement with the constraints from the impact crater excavation measurements [102]. Regional geological studies indicate that at least 5 lava eruption events in the CE3 landing region have filled the northeastern area of the Imbrium basin, forming a basalt layer of ~1 km thick [103]. Therefore, it is likely that there should be more volcanic events in the radar profile that filled the Imbrium basin at a greater depth. However, due to some controversy over the data processing of the low-frequency channel of CE3, further research is needed to constrain the subsurface structures of the Imbrian basalts [104].

The lava flows on the farside of the Moon also have layered structures. The LPR profiles show that the CE4 landing area hosts multiple layers of impact ejecta and basalts [105–108].

Downloaded from https://spj.science.org on October 31, 2023

Multi-stage Imbrian basalts with a thickness of 100 m were found at a depth of more than 130 m, which is consistent with the thickness of the basalts in the Von Kármán impact crater estimated by the crater morphology method [105]. The interpretation of shallow layers above 130 m is still under debate. Some studies believe that the depths of 50 to 130 m still have the characteristics of multi-stage Imbrian basalt [107,108], and it was also argued that this layer might be an impact ejecta [105]. Therefore, more data and analytical methods are needed to verify the subsurface structures of mare basalts on the lunar farside.

Subsurface structures of lunar volcanic complexes

Large volcanic complexes on the lunar nearside are topographic prominences that have a high concentration of various volcanic features on the surface, such as domes, pit craters, cones, and rilles [1,109]. They open an important window to study the thermal evolutionary history of the lunar nearside crust and mantle. Using high-resolution imagery and topographic data, Spudis et al. [110] recognized 8 large volcanic complexes (Marius Hills, Mons Rümker, Prinz, Kepler, Hortensius, Cauchy, Gardner, and Aristarchus) on the nearside of the Moon and suggested that these features were large shield volcanoes equivalent to those on Mars, Earth, and Venus. Six of them are located within the Oceanus Procellarum and the other two are in the Mare Tranquillitatis (Fig. 4).

Subsurface mass density is important to determine the composition of a volcano and at a greater depth to understand the crustal evolution. Without sufficient lunar seismic data, high-resolution gravity data provide an efficient way to detect the subsurface structure of those volcanic complexes. A joint gravity and topography spectral analysis of these regions suggested that the shallow crusts of the Mons Rümker, Marius Hills, Gardner, and Kepler are mainly composed of dense intrusive/extrusive magmatic units, with crustal and surface load densities larger than 2,850 kg m^{-3}, while Aristarchus Plateau and Hortensius are mainly composed of low-density materials with only small amounts of superimposed volcanic material, with lower crustal and load densities of 2,550 kg m^{-3} [111]. Using gravity forward modeling methods, both Kiefer [112] and Deutsch et al. [113] fitted the observed gravity anomaly in the Marius Hills region with a subsurface dense model. The former suggested basaltic intrusions as magma chamber in a feldspathic porous crust, while the latter showed either a dike complex extending from the crust-mantle boundary to the surface or dike complex combined with a mare-filled impact crater beneath the Marius Hills. Evans et al. [114] identified quasi-circular positive gravity anomalies beneath both the Marius Hills and Gardner, and suggested buried impact craters filled out with dense mare basalts. Zhang et al. [115] analyzed both the geomorphology and gravity anomalies of several volcanic complexes, and argued that magmatic intrusions would exist in the crust of Marius Hills, Gardner, and Rümker regions. Applying a 3D density inversion method on Bouguer gravity data, Chisenga et al. [116] obtained the subsurface density structures of the Rümker region and suggested a high-density basalts (>3,000 kg m^{-3}) intrusion with a depth of ~6 to 18 km in the crust.

Hidden structures related to magma intrusion

On the Moon, a single-plate planet, volcanism arose mainly from mantle melting, which formed the source region of lunar basaltic magma located 200 to 400 km below the lunar surface [117]. Magma erupts through the lunar crust to the surface, forming a variety of structures; however, most of the magma did not reach the lunar surface but was preserved by intrusion into the lunar crust [118]. On Earth, the volume of intruded magma is approximately 10 times the volume of extruded lava for the continental crust and 5 times the volume of extruded lava for the oceanic crust [119]. Buoyancy dominates the movement of magma from the interior to the shallow or surface of the planet [120,121]. The latest estimation from the GRAIL mission provides a mean density for the lunar crust that is particularly low, of 2,550 kg/m^3 [12,28]. A large density of magma can be inferred from the density of 3,010 kg/m^3 of lunar mare basalt [122], so the intrusion-to-extrusion ratio on the Moon may be even higher than that on Earth [63,123,124], and can reach an upper limit of 50:1 [118].

While remote sensing imaging and spectral data are used to study volcanic features on the lunar surface, gravity data provide important supplements for us to investigate hidden structures related to magma intrusion. The latest model produced by Goossens et al. [125] has been solved to the degree 1,500. The information in the degree 60 to 600 is commonly used for lunar crust range studies, which have removed long-wavelength effects and noise from the high-degree coefficients. The degree 60 corresponds to the depth of ~30 km beneath the lunar surface, and the degrees <600 represent the completely resolved coefficients according to the real satellite tracking data [126,127]. Further combined with the 3D density inversion model [128], the 3D density spatial information within the lunar crust can be obtained. The GRAIL field reveals the fine details of subsurface structure for volcanism, including tectonic structures and mafic instructions. For example, huge dikes were discovered surrounding the Procellarum KREEP Terrane with a length of thousands of kilometers where ancient magma may erupt [129]. In addition, gravity measurements also revealed lunar mass concentrations, or "mascons" associated with impact basins [130,131]. However, the lava emplacement of the mare basalts cannot create such a large-gravity central positive anomaly in the basin, nor can the central positive anomaly be surrounded by concentric negative anomalies [132,133]. The gravity anomaly structure of the lunar mascon basin is attributed to mantle rebound and thickened crust [132,134]. The impact event thinned the lunar crust and magma from the mantle intruded into the crust, which provided favorable conditions for subsequent volcanism. Some of the mascons reveal the existence of buried basins in which cryptovolcanism and cryptomaria have been identified [135]. Depending on assumptions about density and crustal compensation state, the volume of the candidate buried cryptovolcanic deposits was estimated. These candidate deposits correspond to a surface area of between 0.50×10^6 km^2 and 1.14×10^6 km^2, which would increase the amount of the lunar surface containing volcanic deposits from 16.6% to between 17.9% and 19.5% [135].

Outstanding Problems and Future Exploration Targets

The temporal and spatial span of lunar volcanism

In recent years, an outstanding issue of lunar exploration is how long such a small terrestrial planetary body can sustain volcanic activity. Addressing this issue can provide new insights

Downloaded from https://spj.science.org on October 31, 2023

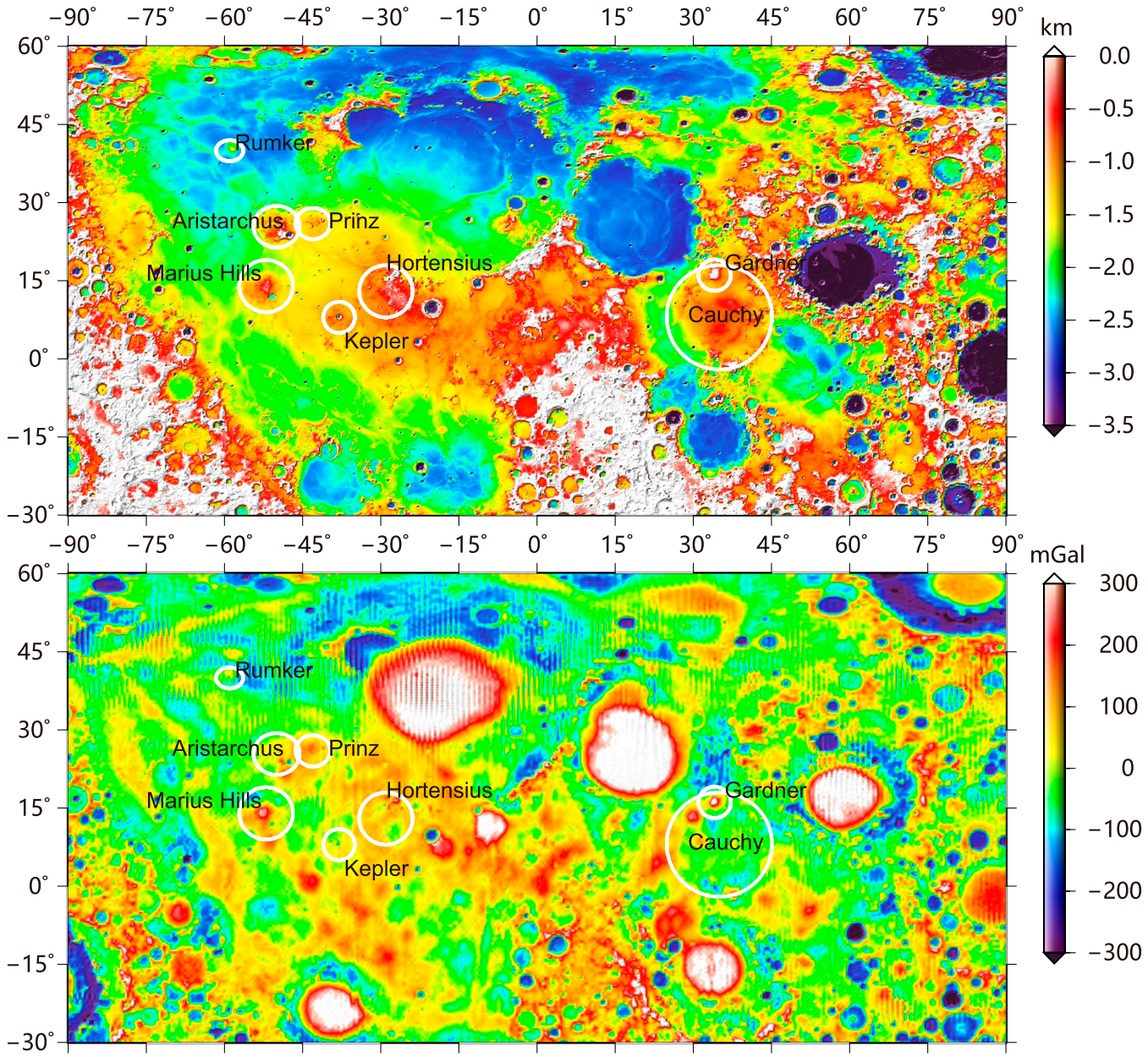

Fig. 4. Topography (top) and gravity map (bottom) of the lunar nearside. The white circles indicate the locations of 8 large volcanic complexes proposed by Spudis et al. [110]. The topographic map is derived from the LOLA 2050 spherical harmonic model (lro_ltm05_2050_sha.tab, http://pds-geosciences.wustl.edu/lro/lro-l-lola-3-rdr-v1/lrolol_1xxx/data/lola_shadr/) and the free-air gravity is from the newly released GL1500E model (jggrx_1500e_sha.tab, https://pds-geosciences.wustl.edu/grail/grail-llgrs-5-rdr-v1/grail_1001/) [126]. This figure is in a cylinder equidistant projection.

into and constrain our current models of the thermal and compositional evolution of the Moon [80]. However, the start and end of lunar volcanic activity are still waiting to be confirmed. Studying returned samples of lunar mare basalts indicates volcanism with a time range of ~3.8 to 3.1 Ga [136] and the youngest known age of ~2.0 Ga [137,138], while lunar meteorites record the oldest mare basalt volcanism starting as early as ~4.35 Ga [31,139]. High-silicic volcanism on the Moon was also dated to occur at this time period between ~2.0 and 4.32 Ga [64,140,141]. Crater counting work, however, implies that mare volcanism on the Moon continued until ~1.2 Ga ago [30], and even much younger than the age by characterizing small volcanic features in the lunar maria based on remotely acquired data [73,76,82].

To confidently determine the span of lunar volcanism, more samples from the oldest and youngest mare units are required. To locate the potential cryptomeria, remote sensing data are needed to directly identify and characterize the cryptomeria buried by basin ejecta. To collect the potential youngest lunar volcanic deposits, samples from the IMPs [59], RMDS [57], and young mare basalts on the south of Aristarchus Plateau (P60 unit in [30]) or northwest of Kepler crater (U17 unit in [34]) are needed.

In addition, by determining the temporal and spatial span of lunar volcanism, the outstanding questions of (a) the nature and origin of the dichotomy in the distribution of basalts on the lunar nearside and farside, and (b) the mechanism for the emplacement and longevity of lunar volcanism may be solved.

Downloaded from https://spj.science.org on October 31, 2023

Formation mechanism of lunar volcanic landforms

As introduced in the "Styles of Lunar Volcanism and Related Volcanic Landforms" section, the Moon hosts a diversity of volcanic landforms that have been studied using imaging, topographic, spectral, and radar data. Nevertheless, debates still exist concerning the formation mechanism of the landforms. For example, the thermal erosion origin [142] and mechanical erosion origin [143] of sinuous rilles have been long discussed. Hurwitz et al. [144] proposed that the sinuous rilles in the mare region (accounting for 78% of the global lunar sinuous rille population) should have formed mainly by thermal erosion, while those rilles originated in the highlands were likely formed mainly by mechanical erosion, as the highland regolith is much thicker and is expected to be more easily eroded. It is worth noting that the sampling site of China's Chang'e-5 mission is located 17 km west of the longest sinuous rilles on the Moon, Rima Sharp. The large-volume volcanic eruption that formed this sinuous rille may source the mare deposits at the Chang'e-5 sampling site. Analysis of the Chang'e-5 samples is expected to provide key information for the formation mechanism of lunar sinuous rilles [145,146].

In addition, the origin of silica-rich volcanic features is also mysterious without returned samples. Based on radiometer data from Diviner Lunar Radiometer Experiment, silica-rich features were found at Aristarchus, Compton-Belkovich, Gruithuisen, Hansteen Alpha, Helmet, Lassell Massif, and Montes Riphaeus regions, characterized by their high-silicate mineralogy and abundant Th abundances [63,147]. Silicate liquid immiscibility, fractional crystallization, and underplating are the 3 most possible mechanisms to form those non-mare features [25], but no solid conclusions have been drawn yet. Any samples from a typical silica-rich feature like Gruithuisen domes would largely help to constrain the petrogenesis of their origin.

Overall, in situ samples as well as high-quality in situ imaging and radar data are key requirements to constrain the formation mechanism of lunar volcanic landforms.

Subsurface structures of lunar volcanic features

Although gravity and radar data have greatly helped us understand the subsurface structures of lunar volcanic features, several aspects still need to be considered: (a) gravity data do not have inherent depth resolution, and therefore, the vertical or radial distribution of density in the recovered 3D model is a direct consequence of prior information or constraints applied [148]; (b) kilometer-depth structures of lunar mare can be detected using orbital radar or active source moonquake; however, the resolution of these detections is too low to identify finer lava flow and the detection range of moonquake data is very limited; (c) mare basalts should contain different types of deposits [149] such as volcanic ash and pyroclastic; however, the imaging method based on radar waves has not been fully effective to identify them. To solve these problems, improved orbital radars and more moonquake experiments are needed, and dependent data processing and inversion methods of radar and gravity data should be developed for the volcanic features. In addition, deploying both in situ and orbital instruments together could help to compare the data obtained both from the surface and orbit, which would largely help to construct the subsurface of a volcanic feature in various resolutions.

Conclusions

Volcanism links the interior to the surface of the Moon and, thus, serves as a window into the lunar geological and thermal history. Recent researches have better constrained the distribution and duration of lunar volcanism, identified a variety of landforms that related to different volcanic styles, and revealed the deep structure associated to lunar volcanism. We analyzed these advances, and proposed that problems still exist on the spatial and temporal span as well as the emplacement of lunar volcanism, the formation mechanism of some lunar volcanic landforms such as sinuous rilles and silica-rich domes, and the fine subsurface structures of lunar volcanic features. To solve these questions, the most important demand is to acquire more lunar samples and high-quality in situ data of typical lunar volcanic features. We believe that with the continuous implementation of China's lunar exploration program, more secrets of lunar volcanism will be uncovered in the near future.

Acknowledgments

Funding: This study is supported by the National Natural Science Foundation of China (42241111, 42030108, 42241107, 12273044, and 41904119), the China Postdoctoral Science Foundation (2021M702999), the Fundamental Research Funds for the Central Universities (CUG2106122 and CUG2106109), the National Key Research and Development Program of China (2022YFF0503100 and 2021YFA0715100), the Pre-research Project on Civil Aerospace Technologies of CNSA (D020101 and D020204), the Key Research Program of the Chinese Academy of Sciences (KGFZD-145-2023-15), the Science and Technology Development Fund, Macau SAR (0049/2020/A1), the Opening Fund of Key Laboratory of Geological Survey and Evaluation of Ministry of Education (GLAB2022ZR09), Young Scholars Program of Shandong University, Weihai (No. 202207), and the National Natural Science Foundation of China-Academic Divisions of Chinese Academy of Sciences Frontier Interdisciplinary Research Strategic Research Joint Funding Project (L2224032 and XK2022DXC004). **Author contributions:** L.X. contributed the central idea. J.Z. refined the ideas and conducted the literature review. L.X. and Y.Z. supervised the research and were responsible for finalizing the paper. All the authors contributed to the data analyses, manuscript writing, and revision. **Competing interests:** The authors declare that they have no competing interests.

Data Availability

The data used to support the findings of this study are included within the article.

References

1. Head JW III. Lunar volcanism in space and time. *Rev Geophys*. 1976;14(2):265–300.
2. Crawford, IA, Katherine HJ, Mahesh A. Lunar exploration. In: *Encyclopedia of the solar system*. Amsterdam (the Netherlands): Elsevier; 2014. p. 555–579.
3. Barabashov N, Lipskii Y, The first results obtained from photographs of the invisible side of the moon. In: *A source book in astronomy and astrophysics, 1900-1975*. Cambridge (MA): Harvard University Press; 1979. p. 53–55.

Downloaded from https://spj.science.org on October 31, 2023

4. Papike J, Hodges F, Bence A, Cameron M, Rhodes J. Mare basalts: Crystal chemistry, mineralogy, and petrology. *Rev Geophys*. 1976;14(4):475–540.
5. Tartèse R, Anand M, Gattacceca J, Joy KH, Mortimer JI, Pernet-Fisher JF, Russell S, Snape JF, Weiss BP. Constraining the evolutionary history of the moon and the inner solar system: A case for new returned lunar samples. *Space Sci Rev*. 2019;215(8):54.
6. Neal CR, Taylor LA. Petrogenesis of mare basalts: A record of lunar volcanism. *Geochim Cosmochim Acta*. 1992;56(6):2177–2211.
7. Nozette S, Rustan P, Pleasance L, Kordas J, Lewis I, Park H, Priest R, Horan D, Regeon P, Lichtenberg C, et al. The Clementine mission to the moon: Scientific overview. *Science*. 1994;266(5192):1835–1839.
8. Binder AB. Lunar prospector: Overview. *Science*. 1998;281(5382):1475–1476.
9. Kato M, Sasaki S, Takizawa Y, Team KP. The Kaguya mission overview. *Space Sci Rev*. 2010;154:3–19.
10. Vondrak R, Keller J, Chin G, Garvin J. Lunar reconnaissance orbiter (LRO): Observations for lunar exploration and science. *Space Sci Rev*. 2010;150:7–22.
11. Keller J, Petro N, Vondrak R. The lunar reconnaissance orbiter Mission—Six years of science and exploration at the moon. *Icarus*. 2016;273:2–24.
12. Zuber MT, Smith DE, Watkins MM, Asmar SW, Konopliv AS, Lemoine FG, Melosh HJ, Neumann GA, Phillips RJ, Solomon SC, et al. Gravity field of the moon from the gravity recovery and interior laboratory (GRAIL) mission. *Science*. 2013;339(6120):668–671.
13. Goswami J, Annadurai M. Chandrayaan-1: India's first planetary science mission to the moon. *Curr Sci*. 2009;96(4):486–491.
14. Sundararajan V. Overview and technical architecture of India's Chandrayaan-2 mission to the Moon. Paper presented at: 2018 AIAA Aerospace Sciences Meeting; 2018 Jan 8–12; Kissimmee, FL.
15. Ouyang Z, Li C, Zou Y, Zhang H, Lü C, Liu J, Liu J, Zuo W, Su Y, Wen W, et al. Primary scientific results of Chang'E-1 lunar mission. *Sci Chin Earth Sci*. 2010;53:1565–1581.
16. Ouyang Z. Chang'E-2 preliminary results. *Chin J Nat*. 2013;35(6):391–395.
17. Jia Y, Zou Y, Ping J, Xue C, Yan J, Ning Y. The scientific objectives and payloads of Chang'E-4 mission. *Planet Space Sci*. 2018;162:207–215.
18. Wu W, Li C, Zuo W, Zhang H, Liu J, Wen W, Su Y, Ren X, Yan J, Yu D, et al. Lunar farside to be explored by Chang'E-4. *Nat Geosci*. 2019;12(4):222–223.
19. Li C, Zuo W, Wen W, Zeng X, Gao X, Liu Y, Fu Q, Zhang Z, Su Y, Ren X, et al. Overview of the Chang'E-4 mission: Opening the frontier of scientific exploration of the lunar far side. *Space Sci Rev*. 2021;217:1–32.
20. Zhou C, Jia Y, Liu J, Li H, Fan Y, Zhang Z, Liu Y, Jiang Y, Zhou B, He Z, et al. Scientific objectives and payloads of the lunar sample return mission - Chang'E-5. *Adv Space Res*. 2022;69(1):823–836.
21. Liu J, Ouyang Z, Li C, Zou YL. China national moon exploration progress (2001-2010). *Bullet Mineral Petrol Geochem*. 2013;32:544–551.
22. Neal CR. The moon 35 years after Apollo: What's left to learn? *Geochemistry*. 2009;69(1):3–43.
23. Bradley LJ, Mark AW, Charles KS, Clive RN. *New views of the moon*. Berlin, Boston: De Gruyter; 2006.
24. Dhingra D. The new moon: Major advances in lunar science enabled by compositional remote sensing from recent missions. *Geosciences*. 2018;8(12):498.
25. Head JW, Wilson L. Generation, ascent and eruption of magma on the moon: New insights into source depths, magma supply, intrusions and effusive/explosive eruptions (part 2: Predicted emplacement processes and observations). *Icarus*. 2017;283:176–223.
26. Li C, Wang C, Wei Y, Lin Y. China's present and future lunar exploration program. *Science*. 2019;365(6450):238–239.
27. Nelson D, Koeber S, Daud K, Robinson M, Watters T, Banks M, Williams N. Mapping lunar maria extents and lobate scarps using LROC image products. Paper presented at: Lunar and Planetary Science Conference Abstract; 2014 March; Texas.
28. Wieczorek MA, Neumann GA, Nimmo F, Kiefer WS, Taylor GJ, Melosh HJ, Phillips RJ, Solomon SC, Andrews-Hanna JC, Asmar SW, et al. The crust of the moon as seen by GRAIL. *Science*. 2013;339(6120):671–675.
29. Huang J, Xiao Z, Flahaut J, Martinot M, Head J, Xiao X, Xie M, Xiao L. Geological characteristics of Von Kármán crater, northwestern south pole-Aitken Basin: Chang'E-4 landing site region. *J Geophysl Res: Planets*. 2018;123(7):1684–1700.
30. Hiesinger H, Head J, Wolf U, Jaumann R, Neukum G. Ages and stratigraphy of lunar mare basalts: A synthesis. *Rec Adv Curr Res Issues Lunar Stratig*. 2011;477:1–51.
31. Terada K, Anand M, Sokol AK, Bischoff A, Sano Y. Cryptomare magmatism 4.35 Gyr ago recorded in lunar meteorite Kalahari 009. *Nature*. 2007;450(7171):849–852.
32. Whitten JL, Head JW. Lunar cryptomaria: Physical characteristics, distribution, and implications for ancient volcanism. *Icarus*. 2015;247:150–171.
33. Stöffler D, Ryder G. 2001. Stratigraphy and isotope ages of lunar geologic units: Chronological standard for the inner solar system. *Space Sci Rev*. 2001;12(96):9–54.
34. Qian Y, She Z, He Q, Xiao L, Wang Z, Head JW, Sun L, Wang Y, Wu B, Wu X, et al. Mineralogy and chronology of the young mare volcanism in the Procellarum-KREEP-terrane. *Nat Astronomy*. 2023;1–11.
35. Whitten J, Head JW, Staid M, Pieters CM, Mustard J, Clark R, Nettles J, Klima RL, Taylor L. Lunar mare deposits associated with the Orientale impact basin: New insights into mineralogy, history, mode of emplacement, and relation to Orientale Basin evolution from moon mineralogy mapper (M3) data from Chandrayaan-1. *J Geophysl Res: Planets*. 2011;116:E00G09.
36. Ivanov MA, Hiesinger H, van der Bogert CH, Orgel C, Pasckert JH, Head JW. Geologic history of the northern portion of the south pole-Aitken Basin on the moon. *J Geophysl Res: Planets*. 2018;123(10):2585–2612.
37. Wilson L, Head JW. Generation, ascent and eruption of magma on the moon: New insights into source depths, magma supply, intrusions and effusive/explosive eruptions (part 1: Theory). *Icarus*. 2017;283:146–175.
38. Jozwiak LM, Head JW, Zuber MT, Smith DE, Neumann GA. Lunar floor-fractured craters: Classification, distribution, origin and implications for magmatism and shallow crustal structure. *J Geophysl Res: Planets*. 2012;117(E11):E11005.
39. Hall JL, Solomon SC, Head JW. Lunar floor-fractured craters: Evidence for viscous relaxation of crater topography. *J Geophys Res Solid Earth*. 1981;86(B10):9537–9552.

Downloaded from https://spj.science.org on October 31, 2023

40. Dombard AJ, Gillis JJ. Testing the viability of topographic relaxation as a mechanism for the formation of lunar floor-fractured craters. *J Geophysl Res: Planets*. 2001;106(E11):27901–27909.
41. Wilson L, Head JW. Lunar floor-fractured craters: Modes of dike and sill emplacement and implications of gas production and intrusion cooling on surface morphology and structure. *Icarus*. 2018;305:105–122.
42. Wichman R, Schultz P. Floor-fractured craters in Mare Smythii and west of Oceanus Procellarum: Implications of crater modification by viscous relaxation and igneous intrusion models. *J Geophysl Res: Planets*. 1995;100(E10):21201–21218.
43. Purohit S, Gandhi S, Dubey N, Chauhan P. Quantitative validation of formation mechanism of lunar floor fractured craters. Paper presented at: 2021 IEEE International Geoscience and Remote Sensing Symposium IGARSS; 2021 Jul 11–16; Brussels, Belgium.
44. Jozwiak LM, Head JW, Wilson L. Lunar floor-fractured craters as magmatic intrusions: Geometry, modes of emplacement, associated tectonic and volcanic features, and implications for gravity anomalies. *Icarus*. 2015;248:424–447.
45. Thorey C, Michaut C, Wieczorek M. Gravitational signatures of lunar floor-fractured craters. *Earth Planet Sci Lett*. 2015;424:269–279.
46. Salem IB, Sharma M, Kumaresan P, Karthi A, Howari FM, Nazzal Y, Xavier CM. An investigation on the morphological and mineralogical characteristics of Posidonius floor fractured lunar impact crater using lunar remote sensing data. *Remote Sens*. 2022;14(4):814.
47. Head JW, Gifford A. Lunar mare domes: Classification and modes of origin. *Moon Planets*. 1980;22:235–258.
48. Wöhler C, Lena R, Group GLRG. Lunar intrusive domes: Morphometric analysis and laccolith modelling. *Icarus*. 2009;204(2):381–398.
49. Zhao J, Xiao L, Qiao L, Glotch TD, Huang Q. The Mons Rümker volcanic complex of the moon: A candidate landing site for the Chang'E-5 mission. *J Geophys Res: Planets*. 2017;122(7):1419–1442.
50. Wilson L, Head J. Controls on lunar basaltic volcanic eruption structure and morphology: Gas release patterns in sequential eruption phases. *Geophys Res Lett*. 2018;45(12):5852–5859.
51. Schaber GG. Lava flows in Mare Imbrium: Geologic evaluation from Apollo orbital photography. Paper presented at: Lunar and Planetary Science Conference Proceedings; 1973 Mar 5–8; Houston, TX.
52. Schaber GC, Boyce JM, Moore HJ. The scarcity of mappable flow lobes on the lunar maria-Unique morphology of the Imbrium flows. Paper presented at: Lunar and Planetary Science Conference Proceedings; 1976 Mar 15–19; Houston, TX.
53. Zhang J, Yang W, Hu S, Lin Y, Fang G, Li C, Peng W, Zhu S, He Z, Zhou B, et al. Volcanic history of the Imbrium basin: A close-up view from the lunar rover Yutu. *Proc Natl Acad Sci*. 2015;112(17):5342–5347.
54. Hiesinger H, Jaumann R, Neukum G, Head JW III. Ages of mare basalts on the lunar nearside. *J Geophys Res: Planets*. 2000;105(E12):29239–29275.
55. Wu Y, Li L, Luo X, Lu Y, Chen Y, Pieters CM, Basilevsky AT, Head JW. Geology, tectonism and composition of the northwest Imbrium region. *Icarus*. 2018;303:67–90.
56. Chen Y, Li C, Ren X, Liu J, Wu Y, Lu Y, Cai W, Zhang X. The thickness and volume of young basalts within Mare Imbrium. *J Geophys Res: Planets*. 2018;123(2):630–645.
57. Zhang F, Head JW, Wöhler C, Bugiolacchi R, Wilson L, Basilevsky AT, Grumpe A, Zou Y. Ring-moat dome structures (RMDSs) in the lunar maria: Statistical, compositional, and morphological characterization and assessment of theories of origin. *J Geophys Res: Planets*. 2020;125(7):e2019JE005967.
58. Hurwitz DM, Head JW, Hiesinger H. Lunar sinuous rilles: Distribution, characteristics, and implications for their origin. *Planet Space Sci*. 2013;79:1–38.
59. Qiao L, Head JW, Ling Z, Wilson L. Lunar irregular mare patches: Classification, characteristics, geologic settings, updated catalog, origin, and outstanding questions. *J Geophysl Res: Planets*. 2020;125(7):e2019JE006362.
60. Weitz CM, Head JW III. Spectral properties of the Marius Hills volcanic complex and implications for the formation of lunar domes and cones. *J Geophys Res: Planets*. 1999;104(E8):18933–18956.
61. Huang Q, Zhao J, Wang X, Wang T, Zhang F, Qiao L, Chen Y, Qiu D, Yang Y, Xiao L. A large long-lived central-vent volcano in the Gardner region: Implications for the volcanic history of the nearside of the moon. *Earth Planet Sci Lett*. 2020;542:116301.
62. Wan S, Qiao L, Ling Z. Identification and geomorphometric characterization of volcanic cones in the Marius Hills, the moon. *J Geophys Res: Planets*. 2022;127(11):e2022JE007207.
63. Glotch TD, Lucey PG, Bandfield JL, Greenhagen BT, Thomas IR, Elphic RC, Bowles N, Wyatt MB, Allen CC, Hanna KD, et al. Highly silicic compositions on the moon. *Science*. 2010;329(5998):1510–1513.
64. Ivanov M, Head J, Bystrov A. The lunar Gruithuisen silicic extrusive domes: Topographic configuration, morphology, ages, and internal structure. *Icarus*. 2016;273:262–283.
65. Chen Y, Huang Q, Zhao J, Hu X. Unsupervised machine learning on domes in the lunar Gardner region: Implications for dome classification and local magmatic activities on the moon. *Remote Sens*. 2021;13(5):845.
66. Peterson DW, Holcomb RT, Tilling RI, Christiansen RL. Development of lava tubes in the light of observations at Mauna ulu, Kilauea volcano Hawaii. *Bullet Volcanol*. 1994;56:343–360.
67. Byrnes JM, Crown DA. Morphology, stratigraphy, and surface roughness properties of Venusian lava flow fields. *J Geophys Res: Planets*. 2002;107(E10):91–922.
68. Zhao J, Huang J, Kraft MD, Xiao L, Jiang Y. Ridge-like lava tube systems in southeast Tharsis, Mars. *Geomorphol*. 2017;295:831–839.
69. Coombs CR, Hawke B. A search for intact lava tubes on the Moon: Possible lunar base habitats. Paper presented at: NASA. Johnson Space Center, The Second Conference on Lunar Bases and Space Activities of the 21st Century; 1988 Apr 5–7; Houston, TX.
70. Haruyama J, Hioki K, Shirao M, Morota T, Hiesinger H, van der Bogert CH, Miyamoto H, Iwasaki A, Yokota Y, Ohtake M, et al. Possible lunar lava tube skylight observed by SELENE cameras. *Geophys Res Lett*. 2009;36(21):L21206.
71. Wagner RV, Robinson MS. Distribution, formation mechanisms, and significance of lunar pits. *Icarus*. 2014;237:52–60.
72. Xiao L, Huang J, Zhao J, Zhao J. Significance and preliminary proposal for exploring the lunar lava tubes. *Sci Sinica Phys, Mech Astron*. 2018;48(11):119602.
73. Braden S, Stopar J, Robinson M, Lawrence S, Van Der Bogert C, Hiesinger H. Evidence for basaltic volcanism on the moon within the past 100 million years. *Nat Geosci*. 2014;7(11):787–791.

Downloaded from https://spj.science.org on October 31, 2023

74. Whitaker EA. An unusual mare feature. In: *Apollo 15: Preliminary Science Report*. Washington, D.C.: Scientific and Technical Information Office, National Aeronautics and Space Administration; 1972. p. 84.
75. Strain PL, El Baz F. The geology and morphology of Ina. Paper presented at: Proceedings of the 11th Lunar and Planetary Science Conference; 1980 Mar 17–21; Houston, TX.
76. Schultz PH, Staid MI, Pieters CM. Lunar activity from recent gas release. *Nature*. 2006;444(7116):184–186.
77. Garry WB, Robinson MS, Zimbelman JR, Bleacher J, Hawke B, Crumpler L, Braden S, Sato H. The origin of Ina: Evidence for inflated lava flows on the moon. *J Geophys Res: Planets*. 2012;117(E12):E00H31.
78. Carter L, Hawke B, Garry W, Campbell B, Giguere T, Bussey D. Radar observations of lunar hollow terrain. Paper presented at: 44th Annual Lunar and Planetary Science Conference; 2013 Mar 18–22; The Woodlands, TX.
79. Qiao L, Head J, Wilson L, Xiao L, Kreslavsky M, Dufek J. Ina pit crater on the moon: Extrusion of waning-stage lava lake magmatic foam results in extremely young crater retention ages. *Geology*. 2017;45(5):455–458.
80. Qiao L, Head JW, Wilson L, Ling Z. The Cauchy 5 small, low-volume lunar shield volcano: Evidence for volatile exsolution-eruption patterns and type 1/type 2 hybrid irregular Mare patch formation. *J Geophys Res: Planets*. 2020;125(2):e2019JE006171.
81. Zhang F, Head JW, Basilevsky AT, Bugiolacchi R, Komatsu G, Wilson L, Fa W, Zhu MH. Newly discovered ring-moat dome structures in the lunar maria: Possible origins and implications. *Geophys Res Lett*. 2017;44(18):9216–9224.
82. Zhang F, Head JW, Wöhler C, Basilevsky AT, Wilson L, Xie M, Bugiolacchi R, Wilhelm T, Althoff S, Zou YL. The lunar mare ring-moat dome structure (RMDS) age conundrum: Contemporaneous with Imbrian-aged host lava flows or emplaced in the Copernican? *J Geophys Res: Planets*. 2021;126(8):e2021JE006880.
83. Wilson L, Head JW, Zhang F. A theoretical model for the formation of ring moat dome structures: Products of second boiling in lunar basaltic lava flows. *J Volcanol Geotherm Res*. 2019;374:160–180.
84. Garrick-Bethell I, Seritan M. Laccolith model for lunar ring-moat dome structures. Paper presented at: 52nd Lunar and Planetary Science Conference; 2021 Mar 15–19; Virtual.
85. Shearer CK, Hess PC, Wieczorek MA, Pritchard ME, Parmentier EM, Borg LE, Longhi J, Elkins-Tanton LT, Neal CR, Antonenko I. Thermal and magmatic evolution of the moon. *Rev Mineral Geochem*. 2006;60(1):365–518.
86. Gaddis LR, Staid MI, Tyburczy JA, Hawke BR, Petro NE. Compositional analyses of lunar pyroclastic deposits. *Icarus*. 2003;161(2):262–280.
87. Morgan C, Wilson L, Head JW. Formation and dispersal of pyroclasts on the moon: Indicators of lunar magma volatile contents. *J Volcanol Geotherm Res*. 2021;413:107217.
88. Gustafson JO, Bell J III, Gaddis LR, Hawke BR, Giguere TA. Characterization of previously unidentified lunar pyroclastic deposits using lunar reconnaissance orbiter camera data. *J Geophys Res: Planets*. 2012;117(E12):E00H25.
89. Weitz CM, Head JW III, Pieters CM. Lunar regional dark mantle deposits: Geologic, multispectral, and modeling studies. *J Geophys Res: Planets*. 1998;103(E10): 22725–22759.
90. Kovach RL, Watkins JS, Landers T. Active seismic experiment. In: *Apollo 14 Preliminary Science Report*. Washington, D.C.: Scientific and Technical Information Office, National Aeronautics and Space Administration; 1971.
91. Kovach RL, Watkins JS, Talwani P. Active seismic experiment. In: *Apollo 16 Preliminary Science Report*. Washington, D.C.: NASA Lyndon B. Johnson Space Center; 1972.
92. Hodges C, Muehlberger WR, Ulrich GE. Geologic setting of Apollo 16. Paper presented at: Lunar and Planetary Science Conference Proceedings; 1973 Mar 5–8; Houston, TX.
93. Cooper MR, Kovach RL, Watkins JS. Lunar near-surface structure. *Rev Geophys*. 1974;12(3):291–308.
94. Ono T, Oya H. Lunar radar sounder (LRS) experiment on-board the SELENE spacecraft. *Earth Planets Space*. 2000;52(9):629–637.
95. Ono T, Kumamoto A, Yamaguchi Y, Yamaji A, Kobayashi T, Kasahara Y, Oya H. Instrumentation and observation target of the lunar radar sounder (LRS) experiment on-board the SELENE spacecraft. *Earth Planets Space*. 2008;60: 321–332.
96. Ono T, Kumamoto A, Nakagawa H, Yamaguchi Y, Oshigami S, Yamaji A, Kobayashi T, Kasahara Y, Oya H. Lunar radar sounder observations of subsurface layers under the nearside maria of the moon. *Science*. 2009;323(5916): 909–912.
97. Fang G-Y, Zhou B, Ji Y-C, Zhang Q-Y, Shen S-X, Li Y-X, Guan H-F, Tang C-J, Gao Y-Z, Lu W, et al. Lunar penetrating radar onboard the Chang'e-3 mission. *Res Astron Astrophys*. 2014;14(12):1607.
98. Di K, Liu Z, Liu B, Wan W, Peng M, Wang Y, Gou S, Yue Z, Xin X, Jia M. Chang'e-4 lander localization based on multi-source data. *J Remote Sens*. 2019;23(1):177–184.
99. Xiao L, Zhu P, Fang G, Xiao Z, Zou Y, Zhao J, Zhao N, Yuan Y, Qiao L, Zhang X, et al. A young multilayered terrane of the northern Mare Imbrium revealed by Chang'E-3 mission. *Science*. 2015;347(6227):1226–1229.
100. Yuan Y, Zhu P, Zhao N, Xiao L, Garnero E, Xiao Z, Zhao J, Qiao L. The 3-D geological model around Chang'E-3 landing site based on lunar penetrating radar channel 1 data. *Geophys Res Lett*. 2017;44(13):6553–6561.
101. Yuan Y, Wang F, Zhu P, Xiao L, Zhao N. New constraints on the young lava flow profile in the northern Mare Imbrium. *Geophys Res Lett*. 2020;47(16):e2020GL088938.
102. Qiao L, Xiao L, Zhao J, Huang Q. Geological features and magmatic activities history of sinus Iridum, the moon. *Sci Sinica Phys Mech Astron*. 2014;43(11):1370.
103. Thomson BJ, Grosfils EB, Bussey DBJ, Spudis PD. A new technique for estimating the thickness of mare basalts in Imbrium Basin. *Geophys Res Lett*. 2009;36(12).
104. Li C, Xing S, Lauro SE, Su Y, Dai S, Feng J, Cosciotti B, Di Paolo F, Mattei E, Xiao Y. Pitfalls in GPR data interpretation: False reflectors detected in lunar radar cross sections by Chang'e-3. *IEEE Trans Geosci Remote Sens*. 2018;56(3):1325–1335.
105. Zhang J, Zhou B, Lin Y, Zhu M-H, Song H, Dong Z, Gao Y, Di K, Yang W, Lin H. Lunar regolith and substructure at Chang'E-4 landing site in south pole-Aitken basin. *Nat Astron*. 2021;5(1):25–30.
106. Zhang L, Li J, Zeng Z, Xu Y, Liu C, Chen S. Stratigraphy of the Von Kármán crater based on Chang'E-4 lunar penetrating radar data. *Geophys Res Lett*. 2020;47(15): e2020GL088680.
107. Lai J, Xu Y, Bugiolacchi R, Meng X, Xiao L, Xie M, Liu B, Di K, Zhang X, Zhou B. First look by the Yutu-2 rover at the

Downloaded from https://spj.science.org on October 31, 2023

deep subsurface structure at the lunar farside. *Nat Commun*. 2020;11(1):3426.
108. Yuan Y, Zhu P, Xiao L, Huang J, Garnero EJ, Deng J, Wang F, Qian Y, Zhao N, Wang W, et al. Intermittent volcanic activity detected in the Von Kármán crater on the farside of the moon. *Earth Planet Sci Lett*. 2021;569:117062.
109. Whitford-Stark JL, Head JW III. Stratigraphy of Oceanus Procellarum basalts: Sources and styles of emplacement. *J Geophys Res Solid Earth*. 1980;85(B11):6579–6609.
110. Spudis PD, McGovern PJ, Kiefer WS. Large shield volcanoes on the moon. *J Geophys Res: Planets*. 2013;118(5): 1063–1081.
111. Huang Q, Xiao Z, Xiao L. Subsurface structures of large volcanic complexes on the nearside of the moon: A view from GRAIL gravity. *Icarus*. 2014;243:48–57.
112. Kiefer WS. Gravity constraints on the subsurface structure of the Marius Hills: The magmatic plumbing of the largest lunar volcanic dome complex. *J Geophys Res: Planets*. 2013;118(4):733–745.
113. Deutsch AN, Neumann GA, Head JW, Wilson L. GRAIL-identified gravity anomalies in Oceanus Procellarum: Insight into subsurface impact and magmatic structures on the moon. *Icarus*. 2019;331:192–208.
114. Evans AJ, Soderblom JM, Andrews-Hanna JC, Solomon SC, Zuber MT. Identification of buried lunar impact craters from GRAIL data and implications for the nearside maria. *Geophys Res Lett*. 2016;43(6):2445–2455.
115. Zhang F, Zhu M-H, Bugiolacchi R, Huang Q, Osinski G, Xiao L, Zou Y. Diversity of basaltic lunar volcanism associated with buried impact structures: Implications for intrusive and extrusive events. *Icarus*. 2018;307:216–234.
116. Chisenga C, Yan J, Zhao J, Atekwana EA, Steffen R. Density structure of the Rümker region in the northern Oceanus Procellarum: Implications for lunar volcanism and landing site selection for the Chang'E-5 mission. *J Geophys Res: Planets*. 2020;125(1):e2019JE005978.
117. Taylor SR. Lunar and terrestrial crusts: A contrast in origin and evolution. *Phys Earth Planet Inter*. 1982;29(3-4):233–241.
118. Head JW III, Wilson L. Lunar mare volcanism: Stratigraphy, eruption conditions, and the evolution of secondary crusts. *Geochim Cosmochim Acta*. 1992;56(6):2155–2175.
119. Crisp JA. Rates of magma emplacement and volcanic output. *J Volcanol Geotherm Res*. 1984;20(3-4):177–211.
120. Rivalta E, Böttinger M, Dahm T. Buoyancy-driven fracture ascent: Experiments in layered gelatine. *J Volcanol Geotherm Res*. 2005;144(1-4):273–285.
121. Taisne B, Tait S. Eruption versus intrusion? Arrest of propagation of constant volume, buoyant, liquid-filled cracks in an elastic, brittle host. *J Geophys Res Solid Earth*. 2009;114(B6):B06202.
122. Kiefer WS, Macke RJ, Britt DT, Irving AJ, Consolmagno GJ. The density and porosity of lunar rocks. *Geophys Res Lett*. 2012;39(7):L072011.
123. Wilson L, Head JW III. Ascent and eruption of basaltic magma on the earth and moon. *J Geophys Res Solid Earth*. 1981;86(B4):2971–3001.
124. Hiesinger H, Head JW III. New views of lunar geoscience: An introduction and overview. *Rev Mineral Geochem*. 2006;60(1):1–81.
125. Goossens S, Sabaka T, Wieczorek M, Neumann G, Mazarico E, Lemoine F, Nicholas J, Smith D, Zuber M. High-resolution gravity field models from GRAIL data and implications for models of the density structure of the Moon's crust. *J Geophys Res: Planets*. 2020;125(2):e2019JE006086.
126. Konopliv AS, Park RS, Yuan DN, Asmar SW, Watkins MM, Williams JG, Fahnestock E, Kruizinga G, Paik M, Strekalov D, et al. High-resolution lunar gravity fields from the GRAIL primary and extended missions. *Geophys Res Lett*. 2014;41(5):1452–1458.
127. Lemoine FG, Goossens S, Sabaka TJ, Nicholas JB, Mazarico E, Rowlands DD, Loomis BD, Chinn DS, Neumann GA, Smith DE, et al. GRGM900C: A degree 900 lunar gravity model from GRAIL primary and extended mission data. *Geophys Res Lett*. 2014;41(10):3382–3389.
128. Li Y, Oldenburg DW. 3-D inversion of gravity data. *Geophysics*. 1998;63(1):109–119.
129. Andrews-Hanna JC, Besserer J, Head JW III, Howett CJ, Kiefer WS, Lucey PJ, McGovern PJ, Melosh HJ, Neumann GA, Phillips RJ. Structure and evolution of the lunar Procellarum region as revealed by GRAIL gravity data. *Nature*. 2014;514(7520):68–71.
130. Muller PM, Sjogren WL. Mascons: Lunar mass concentrations. *Science*. 1968;161(3842):680–684.
131. Melosh H, Freed AM, Johnson BC, Blair DM, Andrews-Hanna JC, Neumann GA, Phillips RJ, Smith DE, Solomon SC, Wieczorek MA, et al. The origin of lunar mascon basins. *Science*. 2013;340(6140):1552–1555.
132. Neumann GA, Zuber MT, Smith DE, Lemoine FG. The lunar crust: Global structure and signature of major basins. *J Geophys Res: Planets*. 1996;101(E7):16841–16863.
133. Neumann GA, Zuber MT, Wieczorek MA, Head JW, Baker DM, Solomon SC, Smith DE, Lemoine FG, Mazarico E, Sabaka TJ, et al. Lunar impact basins revealed by gravity recovery and interior laboratory measurements. *Sci Adv*. 2015;1(9):e1500852.
134. Wieczorek MA, Phillips RJ. Lunar multiring basins and the cratering process. *Icarus*. 1999;139(2):246–259.
135. Sori MM, Zuber MT, Head JW, Kiefer WS. Gravitational search for cryptovolcanism on the moon: Evidence for large volumes of early igneous activity. *Icarus*. 2016;273: 284–295.
136. Nyquist L, Shih C-Y. The isotopic record of lunar volcanism. *Geochim Cosmochim Acta*. 1992;56(6):2213–2234.
137. Li Q, Zhou Q, Liu Y, Xiao Z, Lin Y, Li J, Ma H, Tang G, Guo S, Tang X, et al. Two-billion-year-old volcanism on the moon from Chang'e-5 basalts. *Nature*. 2021;600(7887):54–58.
138. Che X, Nemchin A, Liu D, Long T, Wang C, Norman MD, Joy KH, Tartese R, Head J, Jolliff B, et al. Age and composition of young basalts on the moon, measured from samples returned by Chang'e-5. *Science*. 2021;374(6569):887–890.
139. Snape JF, Davids B, Nemchin AA, Whitehouse MJ, Bellucci JJ. Constraining the timing and sources of volcanism at the Apollo 12 landing site using new Pb isotopic compositions and crystallisation ages. *Chem Geol*. 2018;482:101–112.
140. Wagner R, Head JW III, Wolf U, Neukum G. Lunar red spots: Stratigraphic sequence and ages of domes and plains in the Hansteen and helmet regions on the lunar nearside. *J Geophys Res: Planets*. 2010;115(E6):E06015.
141. Qiu D, Ye M, Yan J, Zheng C, Xiao Z, Zhang Q, Gao W, Liu L, Li F. New view of the lunar silicic volcanism in the Mons Hansteen: Formation and origins. *J Geophys Res: Planets*. 2022;127(8):e2022JE007289.
142. Kerr RC. Thermal erosion of felsic ground by the laminar flow of a basaltic lava, with application to the cave basalt,

Downloaded from https://spj.science.org on October 31, 2023

Mount St. Helens, Washington. *J Geophys Res: Solid Earth*. 2009;114(B9):B09204.
143. Siewert J, Ferlito C. Mechanical erosion by flowing lava. *Contemp Phys*. 2008;49(1):43–54.
144. Hurwitz DM, Head JW, Wilson L, Hiesinger H. Origin of lunar sinuous rilles: Modeling effects of gravity, surface slope, and lava composition on erosion rates during the formation of Rima Prinz. *J Geophys Res: Planets*. 2012;117(E12):E00H14.
145. Qian Y, Xiao L, Head JW, Wilson L. The Long sinuous Rille system in northern Oceanus Procellarum and its relation to the Chang'e-5 returned samples. *Geophys Res Lett*. 2021;48(11):e2021GL092663.
146. Qiao L, Chen J, Xu L, Wan S, Cao H, Li B, Ling Z. Geology of the Chang'e-5 landing site: Constraints on the sources of samples returned from a young nearside mare. *Icarus*. 2021;364:114480.
147. Jolliff BL, Wiseman SA, Lawrence SJ, Tran TN, Robinson MS, Sato H, Hawke BR, Scholten F, Oberst J, Hiesinger H, et al. Non-mare silicic volcanism on the lunar farside at Compton–Belkovich. *Nat Geosci*. 2011;4(8):566–571.
148. Liang Q, Chen C, Li Y. 3-D inversion of gravity data in spherical coordinates with application to the GRAIL data. *J Geophys Res: Planets*. 2014;119(6):1359–1373.
149. Head JW, Wilson L. Rethinking lunar Mare basalt regolith formation: New concepts of lava flow Protolith and evolution of regolith thickness and internal structure. *Geophys Res Lett*. 2020;47(20):e2020GL088334.
150. Head JW, Fassett CI, Kadish SJ, Smith DE, Zuber MT, Neumann GA, Mazarico E. Global distribution of large lunar craters: Implications for resurfacing and impactor populations. *Science*. 2010;329(5998):1504–1507.

Downloaded from https://spj.science.org on October 31, 2023